Journal of Molecular Liquids 280 (2019) 389–398

Contents lists available at ScienceDirect

Journal of Molecular Liquids

journal homepage: www.elsevier.com/locate/molliq

Hydrophilicity of the hydrophobic group: Effect of cosolvents and ions

Dilip H.N., Debashree Chakraborty *

Department of Chemistry, National Institute of Technology Karnataka, Surathkal, Mangalore 575025, Karnataka, India

ARTICLE INFO

Article history:
Received 10 November 2018
Received in revised form 11 January 2019
Accepted 2 February 2019
Available online 10 February 2019

Keywords:
Hydrophobic hydration
Glycine
Trimethylamine N-oxide (TMAO)
Urea
KCl
LiCl
MD simulation

ABSTRACT

Classical molecular dynamics simulations were performed to study the effect of cosolvents and ions on the solvation structure of zwitterionic glycine in liquid water. Simulations were carried out for 2 M and 1 M concentration of TMAO, Urea, KCl and LiCl solutions to observe the changes in liquid structure of water near the glycine molecule. Radial distribution functions and spatial distribution functions showed the presence of protective hydration layer near the C_α in presence of TMAO which gets reduced in case of urea, KCl and minimum in case of LiCl. LiCl is found to disrupt severely the solvation structure near the glycine molecule. For LiCl system, a small hydration layer is found near C_α unit at higher distances which is mainly due to the first hydration shell of lithium ion bonded to the carboxylate group. Presence of these hydration layers gives extra stabilization energy to the glycine water system. Stabilizing and destabilizing effect of water near the glycine molecule is calculated in terms of Potential Mean Force. The anomalous behaviour of lithium salts with respect to Group I cation salts in protein stabilization can be explained on the basis of this behaviour. We found maximum hydrogen bond lifetime for water molecules in presence of TMAO followed by LiCl, KCl and least in case of urea. The higher lifetimes in presence of ions are found mainly due to their electrostatic force. The stabilization of the hydrophobic part of the glycine molecule can be correlated with the stabilization of proteins in presence of these cosolvents.

1. Introduction

Water is unquestionably a complex liquid. It is not a static solvent; it has dynamic micro-domains which result to many anomalous properties. The dynamics of water around biological molecules is complex and non-uniform [1]. Biomolecules modify the structure of the adjacent solvent layer which in turn changes the properties of the biomolecule. All proteins have both hydrophobic and hydrophilic moieties. It has been found that water exists as micro-domains of high density water (HDW, density 1.2 g/ml) and low density water (LDW, density 0.91 g/ml) [2–8]. These micro-domains can be induced due to the presence of hydrophobic and hydrophilic group in the protein moieties [9,10]. The surface water near the protein molecules mainly gets perturbed compared to the bulk due to changes in the hydrogen-bonding network. The associated distortions and loss of tetrahedral symmetry of the interfacial water molecules in turn affect the dynamic properties. It was observed that there is a decrease in entropy and enthalpy when water was mixed with hydrophobic molecules due to enhanced ordering of the solvation water [11]. Direct experimental proof of enhanced ordering is very difficult to get as the important details of dynamic behaviour are masked by both time-averaged and spatially averaged measurements.

The dynamics of water is not only changed due to the presence of biomolecules, it is also affected by the presence of the cosolvents and ions [12–16]. Aqueous salt solutions are natural environments for functioning of biomolecules. Protein solubility can be changed by the addition of salts to the solution [12]. Salts can affect the electrostatic interactions in a solution through charge-charge interactions [17] or by binding the charged groups and neutralizing it [18]. They can also influence the solubility of amino acids and proteins by altering the overall liquid water structure. The functionality of the protein molecules are also affected by the concentration of the salts. Ions differ widely in their effects on the local structure of water [19–22]. Setschenow constants provide useful information about salting-in and salting-out behaviour of salt ions [23]. The behaviour of ions in solutions in general is discussed in terms of kosmotropic (water structure-making) or chaotropic (water structure-breaking) behaviour. It is known fact that small ions tend to cause “salting-out” i.e., reduction of hydrophobic solubilities; whereas large ions tend to cause “salting-in” i.e. increase in nonpolar solubilities [24,25]. This is explained by the fact that smaller ions have higher charge density which leads to strong electrostatic field. This makes the water molecules to be firmly held in their solvation shell. The exchange of the water with the neighbouring shell becomes less probable which reduces the hydrophobic solubilities. They also exert strong orientational effects on water molecules within their first solvation shell. In case of larger ions, there is easy exchange of the water molecules with the neighbouring shells. The different effects of the ions on local structure of water are also mirrored, in terms of their

* Corresponding author.
E-mail address: debashree@nitk.edu.in (D. Chakraborty).

https://doi.org/10.1016/j.molliq.2019.02.007
0167-7322/

Hofmeister effects. An exception to this trend is seen in case of salts containing lithium ion [26–28]. Lithium ion being the smallest ion in the Group I cations is expected to have the most salting out effect. But it has been reported in many cases that lithium ion has more salting-in property in comparison to sodium or potassium ion [26,27].

This anomalous behaviour of lithium ion indicates that consideration of the charge densities alone to describe their Hofmeister effects is not sufficient [18]. Many molecular dynamic simulation studies have been reported on aqueous solution of ions focussing mainly on the calculation of the hydration thermodynamics of the constituent ions [29–32] and their hydration shell structures [24,25,30,33–42]. Recent studies quantified the extent in which salt concentration strengthens the hydrophobic interaction [28,34,43–45]. Therefore, it would be interesting to observe the sensitivity of biological processes in presence of different ions and their changes in the concentration [12,15,46–49].

Changing the conditions of solution affects the thermodynamics of proteins by altering their structural aspects [47,49]. Presence of alcohols, urea and guanidine hydrochloride are found to denature the proteins; while addition of certain amino acids, sucrose, Trimethylamine N-oxide (TMAO) stabilizes it. Urea is found to denature protein by direct [50–53] and indirect mechanism [54,55]. It alters the structure of water molecules [56–59] and thereby encourages the hydrophobic hydration. It can also directly interact with the polar groups of the protein favoring the denatured state. According to the 'two-stage denaturation process' [60,61], denaturation begins with preferential solvation of protein molecule by urea and expulsion of water from the protein solvation shell. TMAO on the other hand, is known to be excluded from the protein surface for entropy effect [62–64]. Its changes on the structure of water lead to stabilization of proteins [65,66]. Several experiments support the formation of immobile water [67–70] in presence of TMAO which is supported by the simulations [71,72]. There are also some studies done on the mixture of urea and TMAO in protein aqueous solutions to study the stabilization effect of TMAO to the protein molecules in presence of urea [73–75]. But the studies of the effect of hydrophobic hydration in presence of these molecules have not been given much importance.

Protein water-exposed interface undergoes a lot of topological disorder and chemical heterogeneity due to presence of hydrophilic and hydrophobic sites. There have been many studies done on the effects of ions on the solvation structure of water, mechanism of urea denaturation on protein, TMAO stabilization, urea and TMAO mixture effect on protein but no systematic study on the role of stabilizing and destabilizing effect of cosolvents on biomolecules. Both urea and concentrated salt solutions are found to denature the protein. Therefore, it would be interesting to see whether there is a common factor between these cosolvents that can explain the reasons leading to the destabilization on the biomolecules and also if it is different from the TMAO effect on the biomolecule. To study this process, we selected a small amino acid, glycine for its simplicity in having one —NH_2 group, one —COOH unit and a hydrophobic part. The hydrophobic group is surrounded by hydrophilic groups. Glycine forms zwitterionic state in aqueous solution and in crystalline state [76–78] whereas; neutral form in the gaseous phase [79,80]. Some theoretical studies using ab initio methods have been reported regarding the study of the internal structure of glycine and its interaction with water molecules and ions [81–86].

Further, it would be interesting to spot some interesting behaviour of Lithium salts which can explain the anomalous behaviour of Lithium solutes with respect to other salts [26–28]. In view of this, we present here a relatively comprehensive set of molecular dynamics (MD) simulations of aqueous glycine in presence of TMAO, Urea, KCl, and LiCl at different concentrations. We are mainly interested to see the effect of cosolvents towards the solvation structure of the glycine and calculation of the forces that stabilizes and destabilizes a protein molecule. In order to study the effects of co-solvents and ions in more details, we performed the simulation in different water models namely, SPC and SPC/E using different thermostat and system size. From this study we can have an overview of basic elementary molecular mechanism that is responsible for protein stabilization. The rest of the paper is organised as follows. Computational methodology is discussed in Section 2 followed by result and discussion in Section 3 and we conclude our results in Section 4.

2. Computational methodology

In the present work, Glycine, Urea, TMAO, KCl, LiCl and water molecules are characterized by multi-site interaction models. In these models, the interaction between atomic sites of two molecules is expressed as

$$u(r_{ij}) = 4\varepsilon_{ij}\left[\left(\frac{\sigma_{ij}}{r_{ij}}\right)^{12} - \left(\frac{\sigma_{ij}}{r_{ij}}\right)^{6}\right] + \frac{q_i q_j}{r_{ij}} \quad (1)$$

where, $r_{ij}$is the distance between sites *i* and j of different molecules, $q_{ij}$is the charge of ith atom and the Lennard-Jones parameter (LJ) $\varepsilon_{ij}$and $\sigma_{ij}$are obtained by using combination rules $\sigma_{ij} = (\sigma_i + \sigma_j)/2$and $\varepsilon_{ij} = \sqrt{\varepsilon_i \varepsilon_j}$, where $\sigma_i$and $\varepsilon_i$are the Lennard-Jones diameter and well-depth parameter for ith atom. For water, we have employed the simple point charge (SPC) model [87] and SPC/E model [88]. The values for the potential parameters for Glycine, Urea, TMAO, KCl, LiCl and water molecules are taken from CHARMM36 FF [89].

The corresponding potential parameters for the amino-acid, co-solvents and water molecules are given in Table 1.

We have carried out classical molecular dynamics in a cubic box comprising a total of 512 and 1024 particles, including zwitterionic glycine, co-solvent and water molecules for SPC and SPC/E water models respectively. The compositions of each solvent mixture in four different solvent systems of varying concentrations are given in Table 2. Simulations were performed using the GROMACS (v2016.5) simulation package [90,91]. The equations of motions were integrated using the leapfrog algorithm with time step of 10^{-15} s (1 fs) along with minimum image conventions and periodic boundary conditions in all three directions [92]. The minimum image conventions for calculation of the short-range Lennard-Jones interactions were employed and the particle mesh Ewald (PME) sum to treat the long-range electrostatic interactions [93,94]. Modified Berendsen thermostat ($\tau_T = 0.1$ ps) [95] and Velocity-rescale ($\tau_T = 0.1$ ps) [96] thermostat was used for SPC and SPC/E water models respectively along with Parrinello-Rahman barostat ($\tau_P = 2.0$ ps) [97] to keep the temperature and pressure constant. All the bonds were constrained using the LINCS algorithm [98].

Table 1
Values of Lennard-jones and electrostatic interaction potential parameters for Glycine, urea, TMAO, KCl, LiCl and water. *e* represents the magnitude of electronic charge.

Name	Atom	$\sigma(A^0)$	ε(kJ/mol)	Charge (*e*)
Glycine	C	3.56	0.2928	0.34
	Cα	3.58	0.2343	0.13
	O	3.02	0.5020	−0.67
	N	3.29	0.8368	−0.30
	H	0.40	0.1924	0.33
	Hα	2.38	0.1171	0.09
Urea	C	3.56	0.2928	0.60
	O	3.02	0.5020	−0.58
	N	3.29	0.8368	−0.69
	H	0.40	0.1924	0.34
TMAO	N	3.29	0.8368	−0.83
	O	3.11	0.5020	−0.37
	C	3.94	0.3221	−0.35
	H	1.24	0.1924	0.25
Water (SPC)	O	3.16	0.6501	−0.82
	H	–	–	0.41
Water (SPC/E)	O	3.16	0.6502	−0.8476
	H	–	–	0.4328

Table 2
$N_{glycine}$, $N_{urea/TMAO/KCl/LiCl}$, N_{water} are the number of glycine, Urea, TMAO, KCl, LiCl and water molecules in the simulation box.[a]

System	$N_{glycine}$	$N_{urea/TMAO/KCl/LiCl}$	N_{water}
1	1	–	511
2	1	10	501(491)
3	1	19	492(473)
4	1	40	983(945)

[a] System 1 corresponds to pure aqueous glycine. System 2 corresponds to 1 M, whereas Systems 3 and 4 correspond to 2 M concentration. SPC water model was used for systems 1,2,3 and SPC/E water model for system 4. Number of water molecules corresponding to KCl and LiCl salts systems are shown in parenthesis.

In the starting configuration, the glycine molecule was centered in the box and co-solvents, water molecules were inserted with random orientations for all the systems. We have carried out simulations in which each system was equilibrated in NVT ensemble for 2 ns, followed by NPT ensemble for 2 ns in order to obtain the appropriate box length corresponding to 1 atm pressure at the end of the simulation. Finally, the simulations were run for another 50 ns and 30 ns for the calculation of the structural and dynamical quantities with 1 fs time step using the NPT ensemble [92] for SPC and SPC/E water models respectively.

3. Results and discussion

3.1. Radial distribution functions

The structural arrangement of water molecules with the variation of solutes around the glycine molecule is calculated from the intermolecular O_w-O_w, C_α-O_w, C-O_w, N_g-O_w and O_g-O_w radial distribution functions (RDF's). Fig. 1 shows the effect of different cosolvents on the RDF of nitrogen of glycine with oxygen of water (N_g-O_w), carbonyl carbon of glycine with oxygens of water (C-O_w), carbonyl-oxygen of glycine with oxygens of water (O_g-O_w), carbonyl oxygen of glycine with cosolvents, hydrophobic carbon of glycine with oxygens of water (C_α-O_w) and water oxygen-oxygen (O_w-O_w) at 2 M concentration for SPC water model. We found similar trend in graph for 1 M SPC and 2 M SPC/E case (Supplementary Figs.1 and 2). It can be observed that the placement of first peak in case of N_g-O_w as shown in Fig. 1(a) is same for all the cosolvent except for LiCl, where the minima are shifted little towards lower distances. The height of the peak is more for urea, TMAO and least for LiCl and KCl, which shows more number of water molecules are bonded with the N-terminal of glycine in case of urea and least in case of ionic solutes. The second coordination shell of urea and pure glycine water remains almost same whereas; the peak height

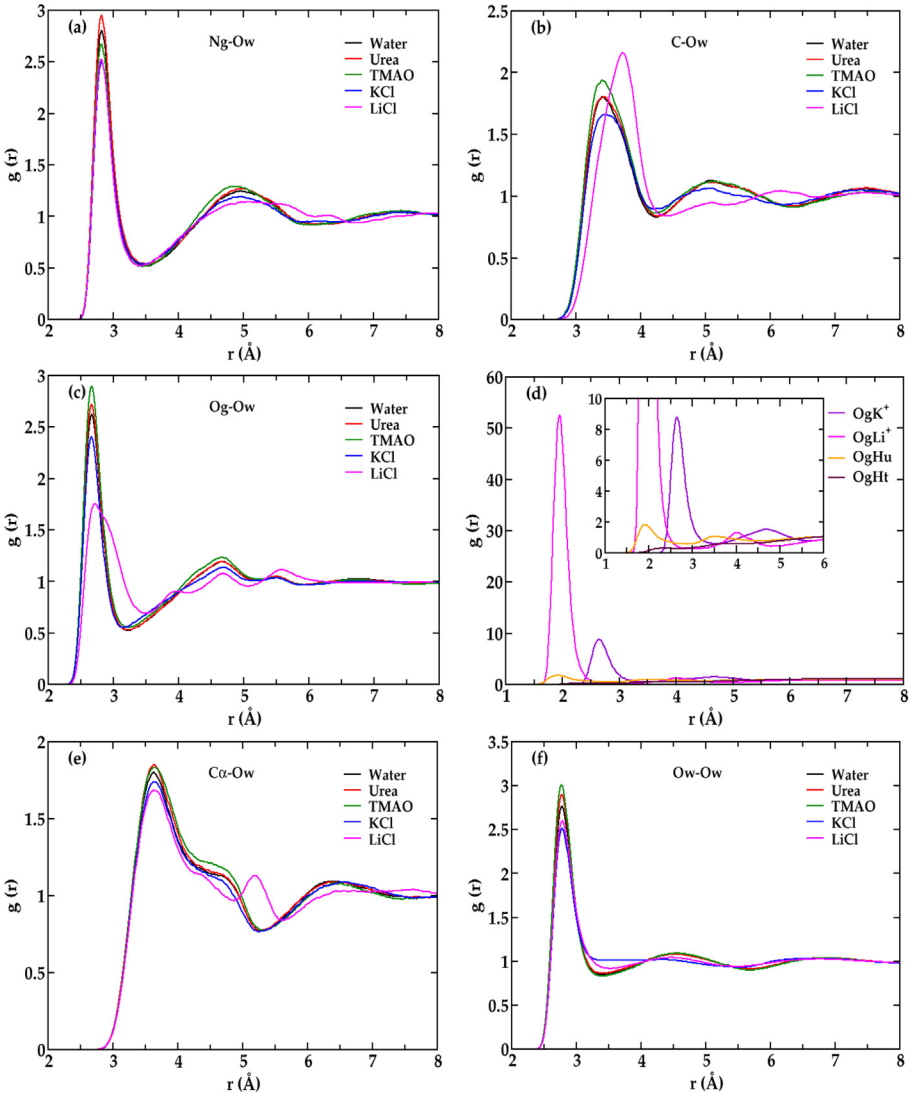

Fig. 1. Radial Distribution functions g(r) of aqueous glycine with different cosolvents for 2 M concentration (a) N_g-O_w, (b) C-O_w, (c) O_g-O_w, (d) O_g with respect to positive ions, hydrogens of urea and TMAO, (e) C_α-O_w and (f) O_w-O_w for SPC water model.

increases slightly for TMAO and much disrupted in case of LiCl. This indicates that the second coordination shell is ordered more for TMAO but as we move towards the ionic salts there is loss in the tetrahedrality of water molecules. We get more well-defined peaks for LiCl in case of SPC/E water model.

The hydration structure of the water molecules near the carbonyl carbon of glycine shown in Fig. 1(b) is found to be more perturbed than the N-terminal in presence of ionic solutes and especially in case of LiCl. The position of the maxima and minima of the first peak is found to be same for TMAO, Urea, KCl and pure glycine water. However, the peak height is found to be more in case of TMAO which reduces in the order of TMAO > urea > KCl. This suggests that water molecules near the carbonyl carbon of glycine are more tetrahedrally ordered in case of TMAO. For LiCl, we observe shifting of the first peak towards higher distances. We also observe significant disruption of the second and third solvation shells for LiCl. Lithium ion has high charge density which significantly changes the structure of the water. The positions of the second and third maxima remain unchanged for TMAO, urea and glycine aqueous solution. However, we observe change in the secondary solvation shell structure for KCl. The structure of the solvation shell for carbonyl oxygen in presence of LiCl shown in Fig. 1(c) is somewhat different from the other three cosolvents. The cations have strong interactions with the carbonyl group compared to urea and TMAO (Fig. 1(d)). In Fig. 2, we have shown the snapshot of the simulation trajectory of aqueous solutions of glycine in the presence of urea, potassium and lithium salts. The radial distribution functions of carboxylate oxygen (O_g)-cosolvent shown in Fig. 1(d) clearly explains the strong association of the lithium cation towards the carbonyl group when compared with potassium ions. It can be noted here that the first maxima of O_g-Li^+ is at 2 Å and that of O_g-O_w in presence of LiCl is at 2.6 Å. The peak height suggests that in case of LiCl, there is more probability of finding Li^+ ions near the surroundings of two carbonyl oxygen atoms than the water molecules. The lithium ion is then surrounded by the water molecules which lead to the shifting of the first solvation shell at higher distances, Fig. 1(c). In case of potassium ion, there is lesser probability of finding K^+ ion near the two carbonyl oxygens in comparison to lithium ion. The first maxima of O_g-K^+ and O_g-O_w are nearly at same distance. Therefore, the changes in the solvation shell of carbonyl oxygen and water molecules (O_g-O_w) for KCl are found to be less pronounced than LiCl. However, the second solvation shell of carbonyl carbon and water oxygen in case of KCl as shown in Fig. 1(b) is seen to be disrupted. In case of urea, we found some probability of binding the hydrogens of urea with carboxylate oxygen at lower distances (Fig. 1(d)) but due to the absence of strong electrostatic field, there is no strong hydration shell near the hydrophobic unit as it is found for LiCl.

The ionic association near the carbonyl oxygen of glycine changes the water density near the hydrophobic unit. It can be seen from Fig. 1(e) that the position of the first maxima is same for all the cosolvents but there is significant difference in the placement of the first minima. The height of the first peak increases in case of TMAO in comparison to aqueous glycine but it decreases in case of the ionic cosolvents. Further, it can be seen that in case of TMAO, we have a small hump near the minima of first solvation shell. The height of the hump decreases from TMAO > urea > KCl > LiCl. This means there is an increment in the density of water molecules near the first solvation of the C_α in case of TMAO compared to aqueous glycine which reduces in case of the ionic solvents. For LiCl, we further notice a smaller hump at a distance of 5.4 Å. The formation of smaller hump can be related to the presence of the first hydration shell of Li^+ ion near the carbonyl oxygen which is missing in case of the other cosolvents. We noticed similar type of hump for SPC/E water model.

Finally, it would be interesting to see the changes in the RDF of the water oxygen-oxygen (O_w-O_w) as shown in Fig. 1(f). The first peak of O_w-O_w RDF profile occurs at 2.80 Å for all of the cosolvents. Variations in the peak height, minima positions and the peak maxima of the second and third solvation shells are observed for all the cases. We observe significant differences in structure of water around the glycine molecule mainly for the ionic cosolvents. The distribution of the peak height of the first maxima clearly shows that the water molecules are more ordered in case of TMAO. Presence of the ions promotes local structure in the water molecules.

Therefore, in the present scenario, we noticed the hydrophobic unit is more surrounded by water molecules in presence of TMAO and LiCl. In other words, it can be said that the hydrophobic part of glycine is more hydrophilic (water loving) in presence of TMAO than other cosolvents. Now, it would be interesting to see whether this hydration of the hydrophobic unit gives an extra stabilization to the glycine water system in comparison to other cosolvent system. For more insights, we have plotted the spatial distribution function in the next section.

3.2. Spatial distribution functions

We have calculated the spatial distribution functions (SDFs) of oxygen molecules around glycine for SPC water model in presence of different co-solvents at 2 M concentration by using the TRAVIS [99] software package. The calculated results of SDFs are shown in Fig. 3. The oxygen atom densities are shown up to 6 Å from the centre of the glycine molecule. It can be seen that there are three main regions where the electron density cloud is mainly distributed. First, near the three hydrogens of the ammonia, second, near the carboxylate ion and third, near the hydrophobic unit. With the change in the cosolvent, we found changes in the electron density mainly near the carboxylate ion and near the hydrophobic unit. The oxygen density near the amine hydrogens remains almost unchanged which correlates well with the RDF results. The oxygen density is significantly more towards the carbonyl group for all the cases mainly due to the strong hydrogen bond between the water molecules with the carbonyl group.

The SDF is found to be same for aqueous glycine and Urea solution, so we have included the plots corresponding to Urea, TMAO, KCl and LiCl in Fig. 3. It can be observed that there is an increment in the oxygen

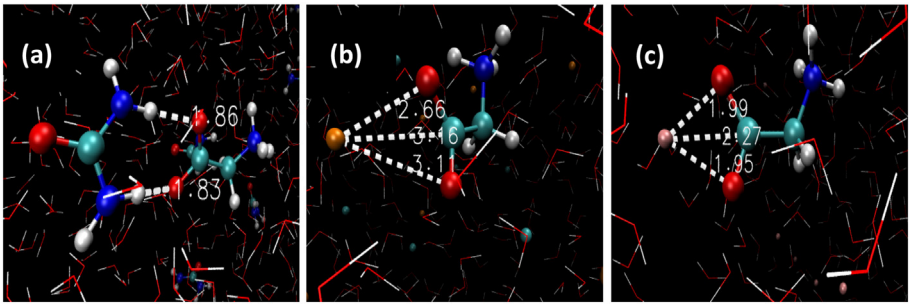

Fig. 2. Snapshots from the simulation of aqueous glycine mixtures in the presence of a) Urea b) KCl c) LiCl at 2 M concentration for SPC water model. Red, green, blue, white, orange and pink spheres represents oxygen, carbon, nitrogen, hydrogen, potassium and lithium atoms respectively. Water molecules are shown in line style. (For interpretation of the references to colour in this figure legend, the reader is referred to the web version of this article.)

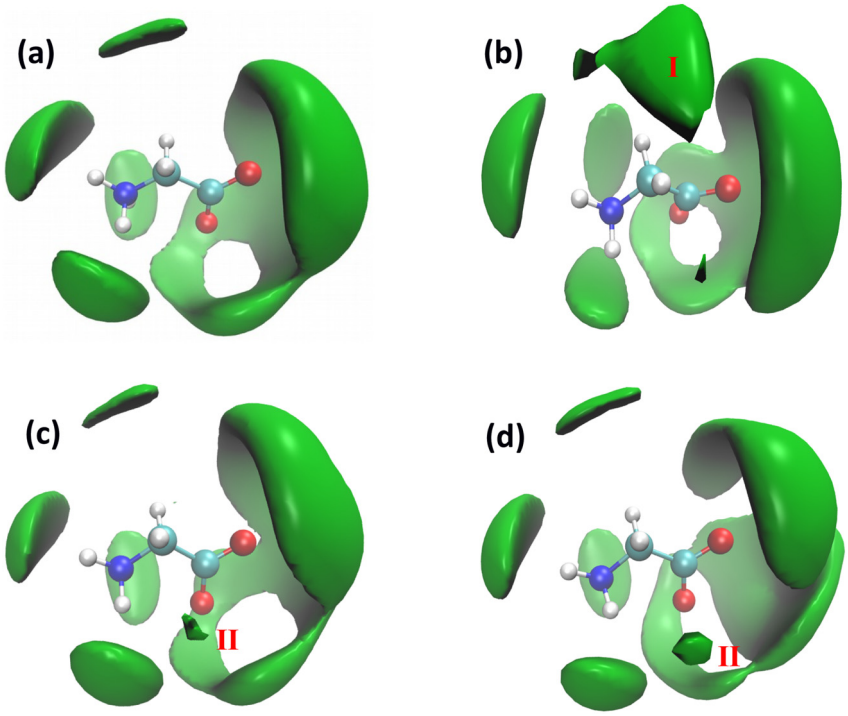

Fig. 3. Spatial distribution functions of the water oxygen around aqueous glycine amino-acid in the presence of different co-solvents (a) Urea, (b) TMAO, (c) KCl and (d) LiCl at 2 M concentration for SPC water model.

density in the region (I) near the hydrophobic unit for TMAO, which is very unique. This is related to the hump seen near the first minima of (C_α-O_w) RDF. Further, it can also be seen that there is a growth of a new water dense region in the region (II) near the carbonyl oxygen for the ions which increases from KCl to LiCl. This can be related to the small hump at 5.4 Å seen in the RDF of hydrophobic carbon of glycine with oxygens of water (C_α-O_w) in case of LiCl.

3.3. Number of hydrogen bonded water molecules

Presence of cosolvents and ions changes the solvent structure near the glycine molecule significantly. Therefore, it would be interesting to see the distribution of water molecules near the interface of amino acid. In Fig. 4, we have plotted the population of number of hydrogen bonded oxygen molecules near the C_α, carbonyl carbon and N-terminal with the variation of cosolvents at 2 M concentration for SPC model.

We have considered 3.25 Å as the distance criteria between two oxygen-oxygen atoms to be hydrogen bonded. We selected only the interfacial water molecules within a distance of 5.6 Å from the C_α, 6.1 Å from carbonyl carbon and 3.5 Å from amine nitrogen of glycine in the calculation. The fraction (f_n) of oxygen atoms of water molecules involving in total *n* number of water–water hydrogen bonds were computed and plotted.

In all of the cases it can be seen that the probability of occurrence of one or two number of hydrogen bonds are found to be more compared to three and four hydrogen bonds. In case of C_α and carbonyl carbon, the probability of three coordinated water molecules are found to be little more in presence of TMAO and LiCl in the solution; whereas presence of KCl and Urea makes the probability of finding single coordinated water more. This indicates that TMAO and LiCl are found to have more ordered water molecules near the C_α of glycine compared to normal glycine water. Presence of KCl and Urea in the solution was found to promote more broken type of hydrogen bonds. Moreover, it can be noticed here that LiCl has more probability of having four coordinated water for carbonyl carbon than TMAO. This can be explained as, since the carbonyl oxygens are more chelated by the Li^+ ion (Fig. 1(d)), there is a probability of finding strongly bound hydration sphere of Li^+ ion. This makes the water molecules more ordered and four coordinated near the carbonyl oxygen. This hydration sphere is missing in case of TMAO and Urea. For K^+ ion even though, there is a probability of finding such hydration sphere near the carbonyl oxygen, it is less likely to be found (Fig. 1(d)).

The scenario is quite different near the N-terminal. All the cosolvents are found to have less ordered and broken hydrogen bonds in comparison to that of pure glycine water. This may be because the anions present in case of the ionic solutes and the oxygen present in TMAO preferably replaces some water molecules near the —NH_2 group (Fig. 1(a)) resulting to lesser number of hydrogen bonded water molecules. For SPC/E water model we found more 3 and 4 number of hydrogen bonds in presence of TMAO near C_α and carbonyl carbon atoms. The rest of the co-solvents behaved in similar way.

3.4. Orientation profile

As evident from the RDF, the structure of the water molecules are very much different near the C-terminal of glycine in presence of different cosolvents, therefore, it would be interesting to see the orientation profile of the water molecules found near the interfaces. One of the important criteria to see the tetrahedrality of the water molecules is to calculate the <O—O—O angle distribution. For tetrahedral water, we know the ideal angle is 104.5°. In Fig. 5, we have plotted the probability distribution of <O—O—O angle of the bulk water and interfacial water molecules near the C_α and the carbonyl carbon at 2 M concentration for SPC water model. We have considered water molecules up to a distance of 5.6 Å from C_α and 6.1 Å from carbonyl carbon as interfacial water molecules. It can be seen that in all the cases we have a broad distribution of angles near 104.5° and a small peak near 50°. These peaks are found to be shifted slightly towards the lower angles in case of ionic cosolvents. Therefore, it can be remarked here that as the cosolvent water hydrogen bond strength decreases compare to water-water hydrogen bond strength, the distribution of <O—O—O angle is found to

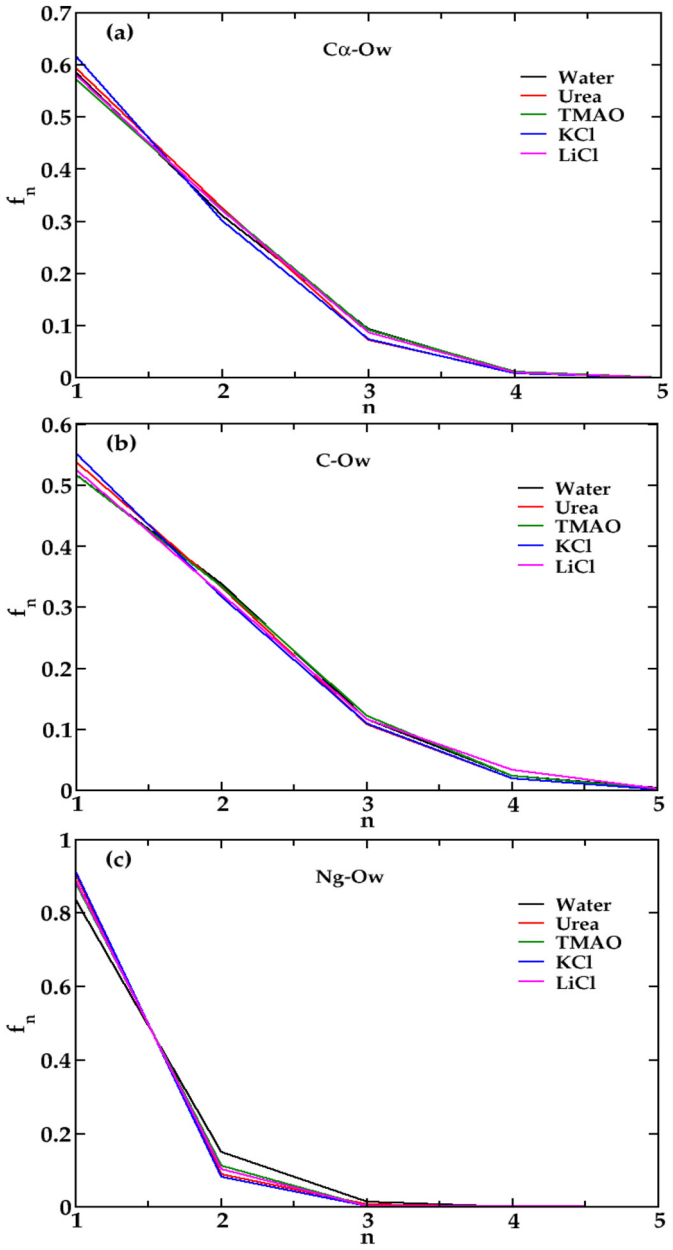

Fig. 4. The fraction of water molecules having n number of hydrogen bonds within the distance (a) 5.6 Å from C_α (b) 6.1 Å from carbonyl carbon and (c) 3.5 Å from amine nitrogen of glycine at 2 M concentration for SPC water model.

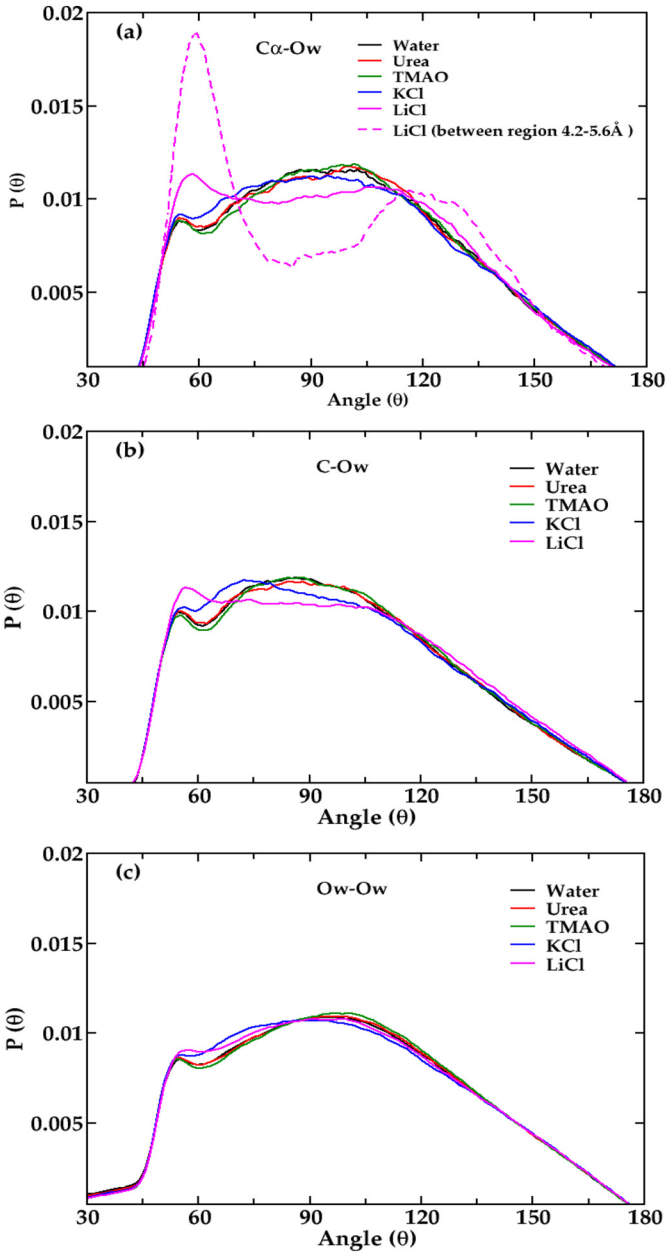

Fig. 5. Probability distribution of <O—O—O angle of oxygen atoms of water molecules which are within distance (a) (a) 5.6 Å from C_α (b) 6.1 Å from carbonyl carbon and (c) bulk O_w at 2 M concentration for SPC water model.

be shifted towards the higher angles. We found similar trend in peak distribution for the interfacial water near C_α (Fig. 5(a)) and carbonyl carbon (Fig. 5(b)). For LiCl, it is found that the distribution near 104.5° gets flat and broader. The peak height near 50° increases. We have also calculated the angle distribution of the water molecules present near the hump region of the C_α carbon for all the cosolvents, i.e., in the distance range of 4.2–5.6 Å, corresponding to the shoulder of the first peak and rise of the second peak. We found similar trend in the graph (Supplementary Fig. 4) as reported in the Fig. 5(a) and 5(b), just the distribution gets broader in the range of 104.5° for all the cosolvents except for LiCl. We found significantly different curve for LiCl and it is included in the Fig. 5(a). It can be seen that there is clear emergence of two peaks in this region for LiCl. Water molecules near the minima of the first solvation shell of the hydrophobic unit in presence of LiCl show two distinct peaks, one at lower angles and the other at the higher angles. This implies that the probability of observing linear hydrogen bonds in this region is very less. The higher charge density of Li^+ ion makes the hydrogen bond strength of the water molecules within the first coordination shell of Li^+ much stronger than the hydrogen bond strength of the water-water molecules which leads to the disruption of the hydrogen bond network and breaking down of the tetrahedral structure to icosahedral structure [100]. The peaks shift from 50° to 60° and emergence of a new peak near 120° occurs. Similar type of behaviour is observed in case of SPC/E water model (Supplementary Fig. 6) except the peaks are broader for LiCl. This implies that the tetrahedral structure of the water molecules are less disturbed in presence of LiCl for SPC/E model as compared to SPC model.

3.5. Potential mean force

Determination of solvation free energies is one of the important criteria in the calculation of stabilizing forces. Solvation energies have

profound influences in the conformational stability. From the calculation of the solvent free energies, we can have an overview of the complex processes that determines the thermodynamics of the biological systems. The structuring of the liquid around the biomolecules adds up a contribution to the free energy cost due to the increased free energy barrier along the potential of mean force between the first and second solvation shells.

To calculate Potential Mean Force (PMF), we have used glycine-water pair correlation functions, g(r), in the equation:

$$W(r) = -k_B T \ln g(r) \quad (2)$$

where, k_B is the Boltzmann constant, T is the temperature and r is the inter-atomic separations.

The differences in PMF can be compared more prominently by converting the first minima and second maxima of the RDF's into free energies. Fig. 6 (a) and (b) shows the relative free energies of interaction between C_α of glycine with the water molecules and carbonyl oxygen with the water molecules at different distances with respect to the interaction energy of the aqueous glycine water respectively for SPC water model.

The concentration considered here is 2 M. A clear difference was found in the interaction of the water molecules with the glycine in presence of different cosolvents. At smaller distances, we found maximum stabilization energy for water molecules near C_α of glycine in presence of TMAO. The stabilization energy decreases as we go towards the more charge dense species (urea > KCl > LiCl). This indicates that water molecules like to come closer to the hydrophobic unit in case of TMAO solution and prefer least in case of LiCl solution. This trend continues up to a distance of 4.8 Å, and then at 5.4 Å for LiCl, we notice a sudden reversal in the trend. At this distance, the stabilization energy is more for LiCl which is even greater than TMAO and at around 5.8 Å, the stabilization energy becomes almost equal for all the cosolvents. At higher distances, again LiCl system becomes the most destabilized with respect to other cosolvents. It is also noted that from 5.4 Å, for all other cosolvents other than LiCl, the stabilization energy becomes almost equal. This stabilization energy gained around 5.4 Å by the LiCl solution can be attributed due to the carbonyl oxygen molecules which are bonded with the Li^+ cation. It would be more clarified if we observe the relative free energies of interaction between carbonyl oxygen of glycine and the water molecules shown in Fig. 6(b). Here also it can be clearly observed that the stabilization energy is more for TMAO solution at smaller distances but around 3.2 Å and 3.5 Å, LiCl solutions give more stabilization. The solution of ionic species, LiCl and KCl solutions are found to have more stabilizing energies than that of urea and TMAO in this region. The stabilization energy in this region is attributed due to the presence of strongly bound first hydration shell of the cations. Lithium being the most charge dense will have more compact hydration shell leading to the more stabilization energy than potassium ions. Therefore, it can be commented here that the maximum hydrophobic solubility is mainly gained in presence of TMAO solution. Ionic solutions also contribute to the hydrophobic solubility due to the presence of the strongly bound hydration shell arising due to the chelated ion-carboxylate ion. This contribution comes more from the LiCl than KCl which may be the origin of the anomalous property shown by Lithium salts. So, the hydrophobic group of glycine is more hydrophilic in presence of TMAO and LiCl.

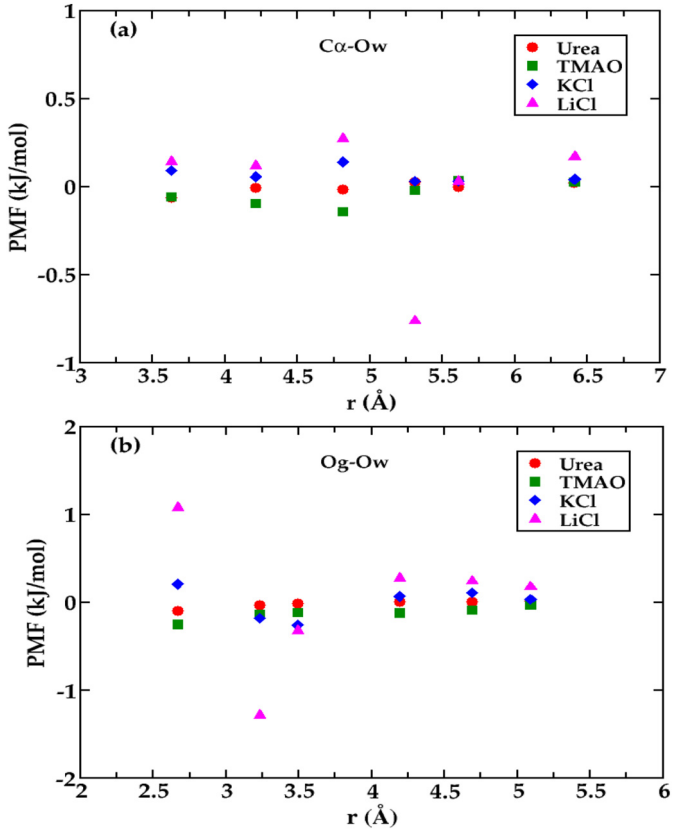

Fig. 6. Potentials of Mean Force depicting the relative free energies of interaction between (a) Hydrophobic carbon, C_α and (b) carbonyl oxygens, O_g of glycine with the oxygen sites of water molecules at different distances with respect to the interaction energy of the aqueous glycine water at 2 M concentration for SPC water model.

3.6. Hydrogen bond dynamics

Since the interaction with the water molecules is one of the main factors of protein stability, therefore it would be interesting to investigate the hydrogen bond strength of the water molecules in presence of these cosolvents. We define two water molecules to be hydrogen bonded if the intermolecular hydrogen-oxygen distance are <2.45 Å. The hydrogen bond population variable H (t) is calculated as follows: If two molecules remain continuously hydrogen bonded from time $t = 0$ to t = t then H (t) = 1 or it is zero otherwise. The continuous correlation function $S_{HB}(t)$ is defined as [101,102]

$$S_{HB}(t) = \frac{\langle h(0)H(t)\rangle}{\langle h(0)^2\rangle} \quad (3)$$

where ⟨...⟩ denotes an average over all pairs of a given type. This function gives the probability that an initially hydrogen bonded pair remains bonded at all times up to t. The associated integrated relaxation time τ_{HB} gives the average hydrogen bond lifetime of that particular pair type. In Table 3, we have given the hydrogen bond lifetime calculated for different cosolvent systems at the interface of the glycine molecule near the amino group, C_α and carbonyl

Table 3
The lifetime (τ_{HB}) of glycine-water and water-water hydrogen bonds (in ps) in the presence of different cosolvents for 2 M and 1 M concentrations for SPC and 2 M concentration for SPC/E water models.[a]

	GW	GUW	GTW	GKClW	GLiClW
(SPC)					
H_{ng}-O_w (τ_{HB})	0.92	0.96(0.94)	1.20(1.04)	1.02(0.97)	1.05(0.98)
O_g-H_w (τ_{HB})	0.93	0.95(0.95)	1.31(1.18)	1.06(0.99)	1.02(1.03)
O_w-H_w (τ_{HB})	0.91	0.95(0.93)	1.18(1.03)	0.99(0.95)	1.03(0.96)
(SPC/E)					
H_{ng}-O_w (τ_{HB})	0.99	1.03	1.29	1.07	1.12
O_g-H_w (τ_{HB})	0.94	0.98	1.31	1.04	1.07
O_w-H_w (τ_{HB})	0.95	0.99	1.42	1.06	1.10

[a] The lifetimes (τ_{HB}) of 1 M solutions are given in parenthesis.

oxygen. We have shown the water-water (O_w-H_w), carbonyl oxygens of glycine-water hydrogen (O_g-H_w) and amine hydrogen of glycine-water oxygen (H_{ng}-O_w) hydrogen bond lifetimes.

For all the cases, we found strong hydrogen bond in case of TMAO [103] followed by LiCl, then KCl and least for Urea. In general, we noticed an increase in hydrogen bond lifetimes for SPC/E water model compared to SPC water model. We found increase in the hydrogen bond lifetimes as the concentration of the cosolvent is increased from 1 M to 2 M. The hydrophilic end of TMAO makes a strong hydrogen bond with the water molecules and the presence of hydrophobic group blocks the approach of new water molecules. This reduces the exchange rate of water molecules leading to increased hydrogen bond lifetime of the water molecules for TMAO. The hydrogen bond lifetime of amine-water and carbonyl-water is also found to increase in presence of TMAO. We found less change in the water-water hydrogen bond lifetime in presence of urea. Urea fits well into the hydrogen bond network of water [65,66]. The structure of TMAO is semi spherically symmetric whereas urea is not symmetric. This causes more disorder and disruption of hydrogen bond in the sphere of influence [65] in case of urea whereas for TMAO we find greater spatial ordering. Therefore, in the case of urea we have faster cooperative hydrogen bond rearrangement dynamics which arises due to the possible disruption in the extended hydrogen bond layer around urea [65,66]. This reduces the water-water hydrogen bond lifetime compare to the presence of TMAO. There is negligible change in hydrogen bond lifetime for carbonyl oxygens and water molecules (O_g-H_w) in presence of urea with the increase in the cosolvent concentration.

The lifetime of the water-water hydrogen bonds increases in presence of ions due to the presence of strong hydration sphere around the ions. This result is in accordance with Soto et al. [104] where it has been reported to have an increase in the molar volume in presence of ions and a consequent increase of compressibility of Glycine [105,106]. With the increase in concentration of the ions this lifetime further increases due to more number of ions and their electrostatic field of attraction. We found an increase of life time also in case of the amine-water hydrogen bond. However, it can be noticed here that we found negligible change in the carbonyl oxygen-water lifetime with the increase in the concentration especially for LiCl case. This further confirms the fact that Li^+ has a preference towards binding of the carbonyl carbon which disrupts the water structure in the lower concentration. On further increase in the concentration, there is negligible change in the water structure. For KCl, we do observe some changes in the hydrogen bond lifetime.

4. Summary and conclusions

In this article we investigated the structural and dynamical properties of TMAO, urea, KCl and LiCl solutions as a function of co-solvent concentration on zwitterionic glycine using MD simulation. We studied the structural properties in terms of radial distribution functions, spatial distribution functions and <O—O—O angle distributions. We also calculated the potential mean force and hydrogen bond dynamics for these systems at different concentrations. TMAO was found to impart more tetrahedrality to the structure of water. The water structure near the N-terminal of glycine was found to be less disrupted than the C-terminal. A compact hydration shell was found for TMAO near the hydrophobic group of glycine which reduces when TMAO is replaced by more charge dense species. However, in ionic systems especially for LiCl, we noticed an increment in the water density near the hydrophobic unit at higher distances due to the presence of the first solvation shell of Li^+ ion bounded to the carboxylate group of the glycine. This water density actually found to give extra stability to glycine molecule.

When Ions are incorporated in the solution, the hydration structure around the glycine molecule is significantly modified. Both the ions interfere the first hydration sphere of glycine. Lithium ions showed preference towards binding with carboxylate ions, which displaces water from the first hydration shell of the carboxylate oxygen. This leads to decrease in the hydration number and number of hydrogen bonds near carboxylate ion. The water structure near the carboxylate ion is strongly modified by LiCl giving rise to two extreme peaks in the angular distribution of <O—O—O near 60° and 120°. These peaks suggest that the tetrahedral structure of water molecules is highly disrupted near the C-terminal. Further, we calculate the hydrogen bond strength of the water molecules near the surface of glycine. Addition of the co-solvents found to increase the hydrogen bond strength of water compared to that of pure glycine water. We found increase in water-water hydrogen bond strength in presence of TMAO whereas; urea showed similar strength of hydrogen bond as that of aqueous glycine. Incorporation of ions increases the hydrogen bond lifetime at the interfaces due to strong electrostatic field. Finally, to conclude it is found that the hydrophobic hydration plays a role in the protein stability. TMAO which is known to stabilize protein structures are found to form a hydration shell near the hydrophobic unit. The formation of another hydration shell was observed in case of LiCl due to the presence of the carboxylate group. These hydration shells were found to give some extra stability and have higher hydrogen bond lifetimes. We termed the presence of these hydration shells near the hydrophobic unit as the “Hydrophilicity behaviour of the hydrophobic group”. The anomalous behaviour of lithium ion in comparison to other Group I cations can be explained on the basis on the extra stability gained due to the presence of the hydration layer in comparison to the potassium ion. Our result also stresses out the fact that the hydrophobic solubility can be attributed as one of the reasons for protein stability.

Notes

The Authors declare no competing financial interest.

Acknowledgements

Funding from DST, SERB (ECR/2016/000707) is highly acknowledged. We would also like to thank Department of Chemistry, NITK Surathkal for their constant support.

Appendix A. Supplementary data

Supplementary data to this article can be found online at https://doi.org/10.1016/j.molliq.2019.02.007.

References

[1] N.V. Nucci, M.S. Pometun, A.J. Wand, Site-resolved measurement of water-protein interactions by solution NMR, Nat. Struct. Mol. Biol. 18 (2011) 245–249, https://doi.org/10.1038/nsmb.1955.
[2] M. Vedamuthu, S. Singh, G.W. Robinson, Properties of liquid water: origin of the density anomalies, J. Phys. Chem. 98 (1994) 2222–2230, https://doi.org/10.1021/j100060a002.
[3] O. Mishima, H.E. Stanley, Decompression-induced melting of ice IV and the liquid–liquid transition in water, Nature 392 (1998) 164–168, https://doi.org/10.1038/32386.
[4] A. Wallqvist, Liquid densities and structural properties of molecular models of water, J. Chem. Phys. 102 (16) (1995) 6559–6565.
[5] S. Woutersen, U. Emmeriches, H. Bakker, Femtosecond mid-IR pump-probe spectroscopy of liquid water: evidence for a two-component structure, Science 278 (5338) (1997) 658–660.
[6] A. Nilson, L.G. Petterson, The structural origin of anomalous properties of liquid water, Nat. Commun. 6 (1) (2015).
[7] S. Biswas, D. Chakraborty, B.S. Mallik, Interstitial voids and resultant density of liquid water: a first-principles molecular dynamics study, ACS Omega 3 (2018) 2010–2017, https://doi.org/10.1021/acsomega.7b01996.
[8] P. Poole, F. Sciortino, U. Essmann, H.E. Stanley, Phase behaviour of metastable water, Nature 360 (6402) (1992) 324–328.
[9] M.M. Teeter, Water-protein interactions: theory and experiment, Annu. Rev. Biophys. Biophys. Chem. 20 (1991) 577–600, https://doi.org/10.1146/annurev.bb.20.060191.003045.
[10] B. Schoenborn, Hydration in protein crystallography, Prog. Biophys. Mol. Biol. 64 (1995) 105–119, https://doi.org/10.1016/0079-6107(95)00012-7.

[11] H.S. Frank, M.W. Evans, Free volume and entropy in condensed systems III. Entropy in binary liquid mixtures; partial molal entropy in dilute solutions; structure and thermodynamics in aqueous electrolytes, J. Chem. Phys. 13 (1945) 507–532, https://doi.org/10.1063/1.1723985.

[12] D.R. Robinson, W.P. Jencks, The effect of concentrated salt solutions on the activity coefficient of Acetyltetraglycine ethyl ester, J. Am. Chem. Soc. 87 (1965) 2470–2479, https://doi.org/10.1021/ja01089a029.

[13] M.G. Cacace, E.M. Landau, J.J. Ramsden, The Hofmeister series: salt and solvent effects on interfacial phenomena, Q. Rev. Biophys. 30 (1997) 241–277.

[14] K.D. Collins, M.W. Washabaugh, The Hofmeister effect and the behaviour of water at interfaces, Q. Rev. Biophys. 18 (1985) 323–422.

[15] P.H. Von Hippel, Effects of neutral salts on the structure and conformational stability of macromolecules in solution, Structure and Stability of Biological Macromolecules, 1969.

[16] S.N. Timasheff, G.D. Fasman, Structure and Stability of Biological Macromolecules, Dekker, New York, 1969.

[17] P. Debye, E. Hückel, De la theorie des electrolytes. I. abaissement du point de congelation et phenomenes associes, Phys. Z. 24 (1923) 185–206.

[18] K. Collins, Ions from the Hofmeister series and osmolytes: effects on proteins in solution and in the crystallization process, Methods 34 (2004) 300–311, https://doi.org/10.1016/j.ymeth.2004.03.021.

[19] C.D. Cappa, J.D. Smith, B.M. Messer, R.C. Cohen, R.J. Saykally, The electronic structure of the hydrated proton: a comparative X-ray absorption study of aqueous HCl and NaCl solutions, J. Phys. Chem. B 110 (2006) 1166–1171, https://doi.org/10.1021/jp0534582.

[20] L.-Å. Näslund, D.C. Edwards, P. Wernet, U. Bergmann, H. Ogasawara, L.G.M. Pettersson, S. Myneni, A. Nilsson, X-ray absorption spectroscopy study of the hydrogen bond network in the bulk water of aqueous solutions, J. Phys. Chem. A 109 (2005) 5995–6002, https://doi.org/10.1021/jp050413s.

[21] S. Chowdhuri, A. Chandra, Hydration structure and diffusion of ions in supercooled water: ion size effects, J. Chem. Phys. 118 (2003) 9719–9725, https://doi.org/10.1063/1.1570405.

[22] D. Chakraborty, A. Chandra, Diffusion of ions in supercritical water: dependence on ion size and solvent density and roles of voids and necks, J. Mol. Liq. 162 (2011) 12–19, https://doi.org/10.1016/j.molliq.2011.05.006.

[23] F. Hofmeister, Zur lehre von der wirkung der salze, Arch. Exp. Pathol. Pharmakol. 25 (1888) 1–30.

[24] K.A. Dill, T.M. Truskett, V. Vlachy, B. Hribar-Lee, Modeling water, the hydrophobic effect, and ion solvation, Annu. Rev. Biophys. Biomol. Struct. 34 (2005) 173–199, https://doi.org/10.1146/annurev.biophys.34.040204.144517.

[25] H. Shinto, S. Morisada, K. Higashitani, Potentials of mean force for hydrophilic–hydrophobic solute pairs in water, J. Chem. Eng. Jpn 38 (2005) 465–477, https://doi.org/10.1252/jcej.38.465.

[26] A.M. Hyde, S.L. Zultanski, J.H. Waldman, Y.-L. Zhong, M. Shevlin, F. Peng, General principles and strategies for salting-out informed by the Hofmeister series, Org. Process. Res. Dev. 21 (2017) 1355–1370, https://doi.org/10.1021/acs.oprd.7b00197.

[27] M. Randall, C.F. Failey, The activity coefficient of non-electrolytes in aqueous salt solutions from solubility measurements. The salting-out order of the ions, Chem. Rev. 4 (1927) 285–290, https://doi.org/10.1021/cr60015a004.

[28] A.S. Thomas, A.H. Elcock, Molecular dynamics simulations of hydrophobic associations in aqueous salt solutions indicate a connection between water hydrogen bonding and the Hofmeister effect, J. Am. Chem. Soc. 129 (2007) 14887–14898, https://doi.org/10.1021/ja073097z.

[29] J. Åqvist, Ion-water interaction potentials derived from free energy perturbation simulations, J. Phys. Chem. 94 (1990) 8021–8024, https://doi.org/10.1021/j100384a009.

[30] J. Chandrasekhar, D.C. Spellmeyer, W.L. Jorgensen, Energy component analysis for dilute aqueous solutions of lithium(1+), sodium(1+), fluoride(1-), and chloride(1-) ions, J. Am. Chem. Soc. 106 (1984) 903–910, https://doi.org/10.1021/ja00316a012.

[31] A. Grossfield, P. Ren, J.W. Ponder, Ion solvation thermodynamics from simulation with a polarizable force field, J. Am. Chem. Soc. 125 (2003) 15671–15682, https://doi.org/10.1021/ja037005r.

[32] A.A. Rashin, B. Honig, Reevaluation of the born model of ion hydration, J. Phys. Chem. 89 (1985) 5588–5593, https://doi.org/10.1021/j100272a006.

[33] B. Hribar, N.T. Southall, V. Vlachy, K.A. Dill, How ions affect the structure of water, J. Am. Chem. Soc. 124 (2002) 12302–12311, https://doi.org/10.1021/ja026014h.

[34] A. Kalra, N. Tugcu, S.M. Cramer, S. Garde, Salting-in and salting-out of hydrophobic solutes in aqueous salt solutions, J. Phys. Chem. B 105 (2001) 6380–6386, https://doi.org/10.1021/jp010568.

[35] S. Chowdhuri, A. Chandra, Molecular dynamics simulations of aqueous NaCl and KCl solutions: effects of ion concentration on the single-particle, pair, and collective dynamical properties of ions and water molecules, J. Chem. Phys. 115 (2001) 3732–3741, https://doi.org/10.1063/1.1387447.

[36] H. Du, J.C. Rasaiah, J.D. Miller, Structural and dynamic properties of concentrated alkali halide solutions: a molecular dynamics simulation study, J. Phys. Chem. B 111 (2007) 209–217, https://doi.org/10.1021/jp064659o.

[37] A. Grossfield, Dependence of ion hydration on the sign of the ion's charge, J. Chem. Phys. 122 (2005), 024506. https://doi.org/10.1063/1.1829036.

[38] E. Guàrdia, D. Laria, J. Martí, Hydrogen bond structure and dynamics in aqueous electrolytes at ambient and supercritical conditions, J. Phys. Chem. B 110 (2006) 6332–6338, https://doi.org/10.1021/jp056981p.

[39] K.P. Jensen, W.L. Jorgensen, Halide, ammonium, and alkali metal ion parameters for modeling aqueous solutions, J. Chem. Theory Comput. 2 (2006) 1499–1509, https://doi.org/10.1021/ct600252r.

[40] S. Obst, H. Bradaczek, Molecular dynamics study of the structure and dynamics of the hydration Shell of alkaline and alkaline-earth metal cations, J. Phys. Chem. 100 (1996) 15677–15687, https://doi.org/10.1021/jp961384b.

[41] M. Patra, M. Karttunen, Systematic comparison of force fields for microscopic simulations of NaCl in aqueous solutions: diffusion, free energy of hydration, and structural properties, J. Comput. Chem. 25 (2004) 678–689, https://doi.org/10.1002/jcc.10417.

[42] S. Rajamani, T. Ghosh, S. Garde, Size dependent ion hydration, its asymmetry, and convergence to macroscopic behavior, J. Chem. Phys. 120 (2004) 4457–4466, https://doi.org/10.1063/1.1644536.

[43] T. Ghosh, A. Kalra, S. Garde, On the salt-induced stabilization of pair and many-body hydrophobic interactions, J. Phys. Chem. B 109 (2005) 642–651, https://doi.org/10.1021/jp0475638.

[44] M. Jönsson, M. Skepö, P. Linse, Monte Carlo simulations of the hydrophobic effect in aqueous electrolyte solutions, J. Phys. Chem. B 110 (2006) 8782–8788, https://doi.org/10.1021/jp0604241.

[45] R.L. Mancera, Influence of salt on hydrophobic effects: a molecular dynamics study using the modified hydration-Shell hydrogen-bond model, J. Phys. Chem. B 103 (1999) 3774–3777, https://doi.org/10.1021/jp9900537.

[46] R. Carta, G. Tola, Solubilities of L-cystine, L-tyrosine, L-leucine, and Glycine in aqueous solutions at various pHs and NaCl concentrations, J. Chem. Eng. Data 41 (1996) 414–417, https://doi.org/10.1021/je9501853.

[47] W.D. Kohn, C.M. Kay, R.S. Hodges, Salt effects on protein stability: two-stranded α-helical coiled-coils containing inter- or intrahelical ion pairs, J. Mol. Biol. 267 (1997) 1039–1052, https://doi.org/10.1006/jmbi.1997.0930.

[48] K.K. Lee, C.A. Fitch, J.T.J. Lecomte, E.B. García-Moreno, Electrostatic effects in highly charged proteins: salt sensitivity of pKa values of histidines in staphylococcal nuclease, Biochemistry 41 (2002) 5656–5667, https://doi.org/10.1021/bi0119417.

[49] C.L. Brooks, L. Nilsson, Promotion of helix formation in peptides dissolved in alcohol and water-alcohol mixtures, J. Am. Chem. Soc. 115 (1993) 11034–11035, https://doi.org/10.1021/ja00076a089.

[50] D.W. Bolen, G.D. Rose, Structure and energetics of the hydrogen-bonded backbone in protein folding, Annu. Rev. Biochem. 77 (2008) 339–362, https://doi.org/10.1146/annurev.biochem.77.061306.131357.

[51] M. Auton, L.M.F. Holthauzen, D.W. Bolen, Anatomy of energetic changes accompanying urea-induced protein denaturation, Proc. Natl. Acad. Sci. 104 (2007) 15317–15322, https://doi.org/10.1073/pnas.0706251104.

[52] M. Auton, D.W. Bolen, Predicting the energetics of osmolyte-induced protein folding/unfolding, Proc. Natl. Acad. Sci. 102 (2005) 15065–15068, https://doi.org/10.1073/pnas.0507053102.

[53] S. Lee, Y.L. Shek, T.V. Chalikian, Urea interactions with protein groups: a volumetric study, Biopolymers 93 (2010) 866–879, https://doi.org/10.1002/bip.21478.

[54] H.S. Frank, F. Franks, Structural approach to the solvent power of water for hydrocarbons; urea as a structure breaker, J. Chem. Phys. 48 (1968) 4746–4757, https://doi.org/10.1063/1.1668057.

[55] K.A. Dill, Dominant forces in protein folding, Biochemistry 29 (1990) 7133–7155, https://doi.org/10.1021/bi00483a001.

[56] B.J. Bennion, V. Daggett, The molecular basis for the chemical denaturation of proteins by urea, Proc. Natl. Acad. Sci. 100 (2003) 5142–5147, https://doi.org/10.1073/pnas.0930122100.

[57] V. Daggett, Protein folding—simulation, Chem. Rev. 106 (2006) 1898–1916, https://doi.org/10.1021/cr0404242.

[58] A. Caballero-Herrera, K. Nordstrand, K.D. Berndt, L. Nilsson, Effect of urea on peptide conformation in water: molecular dynamics and experimental characterization, Biophys. J. 89 (2005) 842–857, https://doi.org/10.1529/biophysj.105.061978.

[59] R.D. Mountain, D. Thirumalai, Molecular dynamics simulations of end-to-end contact formation in hydrocarbon chains in water and aqueous urea solution, J. Am. Chem. Soc. 125 (2003) 1950–1957, https://doi.org/10.1021/ja020496f.

[60] L. Hua, R. Zhou, D. Thirumalai, B.J. Berne, Urea denaturation by stronger dispersion interactions with proteins than water implies a 2-stage unfolding, Proc. Natl. Acad. Sci. 105 (2008) 16928–16933, https://doi.org/10.1073/pnas.0808427105.

[61] N. Samanta, D. Das Mahanta, R. Kumar Mitra, Does urea alter the collective hydrogen-bond dynamics in water? A dielectric relaxation study in the terahertz-frequency region, Chem. Asian J. 9 (2014) 3457–3463, https://doi.org/10.1002/asia.201402696.

[62] D.R. Canchi, P. Jayasimha, D.C. Rau, G.I. Makhatadze, A.E. Garcia, Molecular mechanism for the preferential exclusion of TMAO from protein surfaces, J. Phys. Chem. B 116 (2012) 12095–12104, https://doi.org/10.1021/jp304298c.

[63] E.S. Courtenay, M.W. Capp, C.F. Anderson, M.T. Record, Vapor pressure osmometry studies of osmolyte—protein interactions: implications for the action of osmoprotectants in vivo and for the interpretation of "osmotic stress" experiments in vitro†, Biochemistry 39 (2000) 4455–4471, https://doi.org/10.1021/bi992887l.

[64] T.-Y. Lin, S.N. Timasheff, Why do some organisms use a urea-methylamine mixture as osmolyte? Thermodynamic compensation of urea and trimethylamine N-oxide interactions with protein, Biochemistry 33 (1994) 12695–12701, https://doi.org/10.1021/bi00208a021.

[65] Q. Zou, B.J. Bennion, V. Daggett, K.P. Murphy, The molecular mechanism of stabilization of proteins by TMAO and its ability to counteract the effects of urea, J. Am. Chem. Soc. 124 (2002) 1192–1202, https://doi.org/10.1021/ja004206b.

[66] H. Wei, Y. Fan, Y.Q. Gao, Effects of urea, tetramethyl urea, and trimethylamine N-oxide on aqueous solution structure and solvation of protein backbones: a molecular dynamics simulation study, J. Phys. Chem. B 114 (2010) 557–568, https://doi.org/10.1021/jp9084926.

[67] J. Hunger, K.-J. Tielrooij, R. Buchner, M. Bonn, H.J. Bakker, Complex formation in aqueous trimethylamine-N-oxide (TMAO) solutions, J. Phys. Chem. B 116 (2012) 4783–4795, https://doi.org/10.1021/jp212542q.

[68] Y.L.A. Rezus, H.J. Bakker, Observation of immobilized water molecules around hydrophobic groups, Phys. Rev. Lett. 99 (2007)https://doi.org/10.1103/PhysRevLett.99.148301.
[69] Y.L.A. Rezus, H.J. Bakker, Destabilization of the hydrogen-bond structure of water by the Osmolyte trimethylamine N-oxide, J. Phys. Chem. B 113 (2009) 4038–4044, https://doi.org/10.1021/jp805458p.
[70] A. Panuszko, P. Bruździak, J. Zielkiewicz, D. Wyrzykowski, J. Stangret, Effects of urea and trimethylamine N-oxide on the properties of water and the secondary structure of hen egg white lysozyme, J. Phys. Chem. B 113 (2009) 14797–14809, https://doi.org/10.1021/jp904001m.
[71] L. Larini, J.-E. Shea, Double resolution model for studying TMAO/water effective interactions, J. Phys. Chem. B 117 (2013) 13268–13277, https://doi.org/10.1021/jp403635g.
[72] D. Laage, G. Stirnemann, J.T. Hynes, Why water reorientation slows without iceberg formation around hydrophobic solutes, J. Phys. Chem. B 113 (2009) 2428–2435, https://doi.org/10.1021/jp809521t.
[73] S. Paul, G.N. Patey, Structure and interaction in aqueous urea−trimethylamine N-oxide solutions, J. Am. Chem. Soc. 129 (2007) 4476–4482, https://doi.org/10.1021/ja0685506.
[74] C.J. Sahle, M.A. Schroer, I. Juurinen, J. Niskanen, Influence of TMAO and urea on the structure of water studied by inelastic X-ray scattering, Phys. Chem. Chem. Phys. 18 (2016) 16518–16526, https://doi.org/10.1039/C6CP01922F.
[75] D.R. Canchi, A.E. García, Cosolvent effects on protein stability, Annu. Rev. Phys. Chem. 64 (2013) 273–293, https://doi.org/10.1146/annurev-physchem-040412-110156.
[76] G. Albrecht, R.B. Corey, The crystal structure of glycine, J. Am. Chem. Soc. 61 (1939) 1087–1103, https://doi.org/10.1021/ja01874a028.
[77] P.G. Jönsson, Å. Kvick, Precision neutron diffraction structure determination of protein and nucleic acid components. III. The crystal and molecular structure of the amino acid α-glycine, Acta Crystallogr. B Struct. Crystallogr. Cryst. Chem. 28 (1972) 1827–1833, https://doi.org/10.1107/s0567740872005096.
[78] F.R. Tortonda, J.L. Pascual-Ahuir, E. Silla, I. Tuñón, Why is glycine a zwitterion in aqueous solution? A theoretical study of solvent stabilising factors, Chem. Phys. Lett. 260 (1996) 21–26, https://doi.org/10.1016/0009-2614(96)00839-1.
[79] R. Bonaccorsi, P. Palla, J. Tomasi, Conformational energy of glycine in aqueous solutions and relative stability of the zwitterionic and neutral forms. An ab initio study, J. Am. Chem. Soc. 106 (1984) 1945–1950, https://doi.org/10.1021/ja00319a008.
[80] Y. Ding, K. Krogh-Jespersen, The glycine zwitterion does not exist in the gas phase: results from a detailed ab initio electronic structure study, Chem. Phys. Lett. 199 (1992) 261–266, https://doi.org/10.1016/0009-2614(92)80116-S.
[81] F. Jensen, Structure and stability of complexes of glycine and glycine methyl analogs with H+, li+, and Na+, J. Am. Chem. Soc. 114 (1992) 9533–9537, https://doi.org/10.1021/ja00050a036.
[82] J.H. Jensen, M.S. Gordon, On the number of water molecules necessary to stabilize the Glycine zwitterion, J. Am. Chem. Soc. 117 (1995) 8159–8170, https://doi.org/10.1021/ja00136a013.
[83] I. Tuñón, E. Silla, M.F. Ruiz-López, On the tautomerization process of glycine in aqueous solution, Chem. Phys. Lett. 321 (2000) 433–437, https://doi.org/10.1016/S0009-2614(00)00365-1.
[84] C.H. Wong, F. Siu, N. Ma, C. Tsang, A theoretical study of potassium cation-glycine (K+-Gly) interactions, J. Mol. Struct. THEOCHEM 588 (2002) 9–16, https://doi.org/10.1016/S0166-1280(02)00083-0.
[85] A. Chaudhari, P.K. Sahu, S.-L. Lee, Many-body interaction in glycine–(water)3 complex using density functional theory method, J. Chem. Phys. 120 (2004) 170–174, https://doi.org/10.1063/1.1630019.
[86] K. Leung, S.B. Rempe, Ab initio molecular dynamics study of glycine intramolecular proton transfer in water, J. Chem. Phys. 122 (2005) 184506, https://doi.org/10.1063/1.1885445.
[87] H.J.C. Berendsen, J.P.M. Postma, W.F. van Gunsteren, J. Hermans, Interaction models for water in relation to protein hydration, in: B. Pullman (Ed.), Intermolecular Forces, Springer Netherlands, Dordrecht 1981, pp. 331–342, https://doi.org/10.1007/978-94-015-7658-1_21.
[88] H.J.C. Berendsen, J. Grigera, T. Straatsma, The missing term in effective pair potentials, J. Phys. Chem. 91 (24) (1987) 6269–6271.
[89] J.B. Klauda, R.M. Venable, J.A. Freites, J.W. O'Connor, D.J. Tobias, C. Mondragon-Ramirez, I. Vorobyov, A.D. MacKerell, R.W. Pastor, Update of the CHARMM all-atom additive force field for lipids: validation on six lipid types, J. Phys. Chem. B 114 (2010) 7830–7843, https://doi.org/10.1021/jp101759q.
[90] H.J.C. Berendsen, D. van der Spoel, R. van Drunen, GROMACS: a message-passing parallel molecular dynamics implementation, Comput. Phys. Commun. 91 (1995) 43–56, https://doi.org/10.1016/0010-4655(95)00042-E.
[91] D. Van Der Spoel, E. Lindahl, B. Hess, G. Groenhof, A.E. Mark, H.J.C. Berendsen, GROMACS: fast, flexible, and free, J. Comput. Chem. 26 (2005) 1701–1718, https://doi.org/10.1002/jcc.20291.
[92] M.P. Allen, D.J. Tildesley, Computer Simulation of Liquids, Second edition Oxford University Press, 2017.
[93] T. Darden, D. York, L. Pedersen, Particle mesh Ewald: An N·log(N) method for Ewald sums in large systems, J. Chem. Phys. 98 (1993) 10089–10092, https://doi.org/10.1063/1.464397.
[94] U. Essmann, L. Perera, M.L. Berkowitz, T. Darden, H. Lee, L.G. Pedersen, A smooth particle mesh Ewald method, J. Chem. Phys. 103 (1995) 8577–8593, https://doi.org/10.1063/1.470117.
[95] H.J.C. Berendsen, J.P.M. Postma, W.F. van Gunsteren, A. DiNola, J.R. Haak, Molecular dynamics with coupling to an external bath, J. Chem. Phys. 81 (1984) 3684–3690, https://doi.org/10.1063/1.448118.
[96] G. Bussi, D. Donadio, M. Parrinello, Canonical sampling through velocity rescaling, J. Chem. Phys. 126 (2007), 014101. https://doi.org/10.1063/1.2408420.
[97] M. Parrinello, A. Rahman, Crystal structure and pair potentials: a molecular-dynamics study, Phys. Rev. Lett. 45 (14) (1980) 1196–1199.
[98] B. Hess, H. Bekker, H.J.C. Berendsen, J.G.E.M. Fraaije, LINCS: a linear constraint solver for molecular simulations, J. Comput. Chem. 18 (1997) 1463–1472, https://doi.org/10.1002/(SICI)1096-987X(199709)18:12<1463::AID-JCC4>3.0.CO;2-H.
[99] M. Brehm, B. Kirchner, TRAVIS-a free analyzer and visualizer for Monte Carlo and molecular dynamics trajectories, J. Chem. Inf. Model. 4 (2012) F1.
[100] S. Prasad, C. Chakravarty, Solvation of LiCl in model liquids with high to low hydrogen bond strengths, J. Chem. Phys. 146 (2017) 184503, https://doi.org/10.1063/1.4982828.
[101] A. Luzar, D. Chandler, Hydrogen-bond kinetics in liquid water, Nature 379 (1996) 55–57.
[102] A. Chandra, Effects of ion atmosphere on hydrogen-bond dynamics in aqueous electrolyte solutions, Phys. Rev. Lett. 85 (2000) 768–771, https://doi.org/10.1103/PhysRevLett.85.768.
[103] B.J. Bennion, V. Daggett, Counteraction of urea-induced protein denaturation by trimethylamine N-oxide: a chemical chaperone at atomic resolution, Proc. Natl. Acad. Sci. 101 (2004) 6433–6438, https://doi.org/10.1073/pnas.0308633101.
[104] H. Rodríguez, A. Soto, A. Arce, M.K. Khoshkbarchi, Apparent molar volume, isentropic compressibility, refractive index, and viscosity of DL-alanine in aqueous NaCl solutions, J. Solut. Chem. 32 (2003) 53–63, https://doi.org/10.1023/A:1022640715229.
[105] T. Urbic, Ions increase strength of hydrogen bond in water, Chem. Phys. Lett. 610–611 (2014) 159–162, https://doi.org/10.1016/j.cplett.2014.06.054.
[106] S. Park, M.D. Fayer, Hydrogen bond dynamics in aqueous NaBr solutions, Proc. Natl. Acad. Sci. 104 (2007) 16731–16738, https://doi.org/10.1073/pnas.0707824104.